Supplementary Information to

Biologically Relevant Heterodinuclear Iron Manganese Complexes

Michaël Carboni,[§] Martin Clémancey,[§] Florian Molton,[#] Jacques Pécaut,[¶] Colette Lebrun,[¶] Lionel Dubois,[¶] Geneviève Blondin,[§] J.-M. Latour[§]**

[§] Laboratoire de Chimie et Biologie des Métaux-pmb UMR 5249, Université Joseph Fourier – Grenoble 1 / CEA-DSV-iRTSV / CNRS, Grenoble, F-38054, France

[¶] Laboratoire de Reconnaissance Ionique et Chimie de Coordination UMR-E 3, CEA-INAC-SCIB / Université Joseph Fourier – Grenoble 1 / CNRS, Grenoble, F-38054, France.

[#] Université Joseph Fourier Grenoble 1 / CNRS, Département de Chimie Moléculaire, UMR-5250, Laboratoire de Chimie Inorganique Redox, Institut de Chimie Moléculaire de Grenoble FR-CNRS-2607, BP-53, 38041 Grenoble Cedex 9, France.

Electronic composition at zero-field of the ground doublet of compound 2
Figures S1-S11

Electronic composition at zero field of the ground doublet of compound 2.

Composition of the three lowest Kramers doublets (labeled 1-3 upon increasing energy) of complex **2** calculated at zero-field assuming $D_{Fe} = 3.55$ cm^{-1}, $E_{Fe}/D_{Fe} = 0.21$ and $J = 5.72$ cm^{-1}. The basis functions $\left|\left(S_{Fe}=2, S_{Mn}=\frac{5}{2}\right)S, m_S\right\rangle$ are shortened $|S, m_S\rangle$ with the total spin S and the total spin projection m_S ranging from 1/2 to 9/2 and from $-S$ to $+S$, respectively. Only contributions higher than 0.1 are reported. The + (resp. –) sign written in the kets on the left hand side indicates an increase (resp. decrease) in energy due to the action an external magnetic field.

$$\begin{aligned}|1\pm\rangle = 0.942\left|S=\frac{1}{2}, m_S=\pm\frac{1}{2}\right\rangle \pm 0.209\left|S=\frac{3}{2}, m_S=\pm\frac{1}{2}\right\rangle \pm 0.156\left|S=\frac{3}{2}, m_S=\mp\frac{3}{2}\right\rangle \\ -0.194\left|S=\frac{5}{2}, m_S=\pm\frac{1}{2}\right\rangle + \ldots\end{aligned} \tag{S1}$$

$$\begin{aligned}|2\pm\rangle = -0.166\left|S=\frac{1}{2}, m_S=\mp\frac{1}{2}\right\rangle \mp 0.106\left|S=\frac{3}{2}, m_S=\mp\frac{1}{2}\right\rangle \mp 0.966\left|S=\frac{3}{2}, m_S=\pm\frac{3}{2}\right\rangle \\ \mp 0.120\left|S=\frac{5}{2}, m_S=\pm\frac{3}{2}\right\rangle + \ldots\end{aligned} \tag{S2}$$

$$\begin{aligned}|3\pm\rangle = 0.179\left|S=\frac{1}{2}, m_S=\pm\frac{1}{2}\right\rangle \mp 0.946\left|S=\frac{3}{2}, m_S=\pm\frac{1}{2}\right\rangle \pm 0.133\left|S=\frac{3}{2}, m_S=\mp\frac{3}{2}\right\rangle \\ -0.156\left|S=\frac{5}{2}, m_S=\pm\frac{5}{2}\right\rangle \pm 0.145\left|S=\frac{7}{2}, m_S=\pm\frac{1}{2}\right\rangle + \ldots\end{aligned} \tag{S3}$$

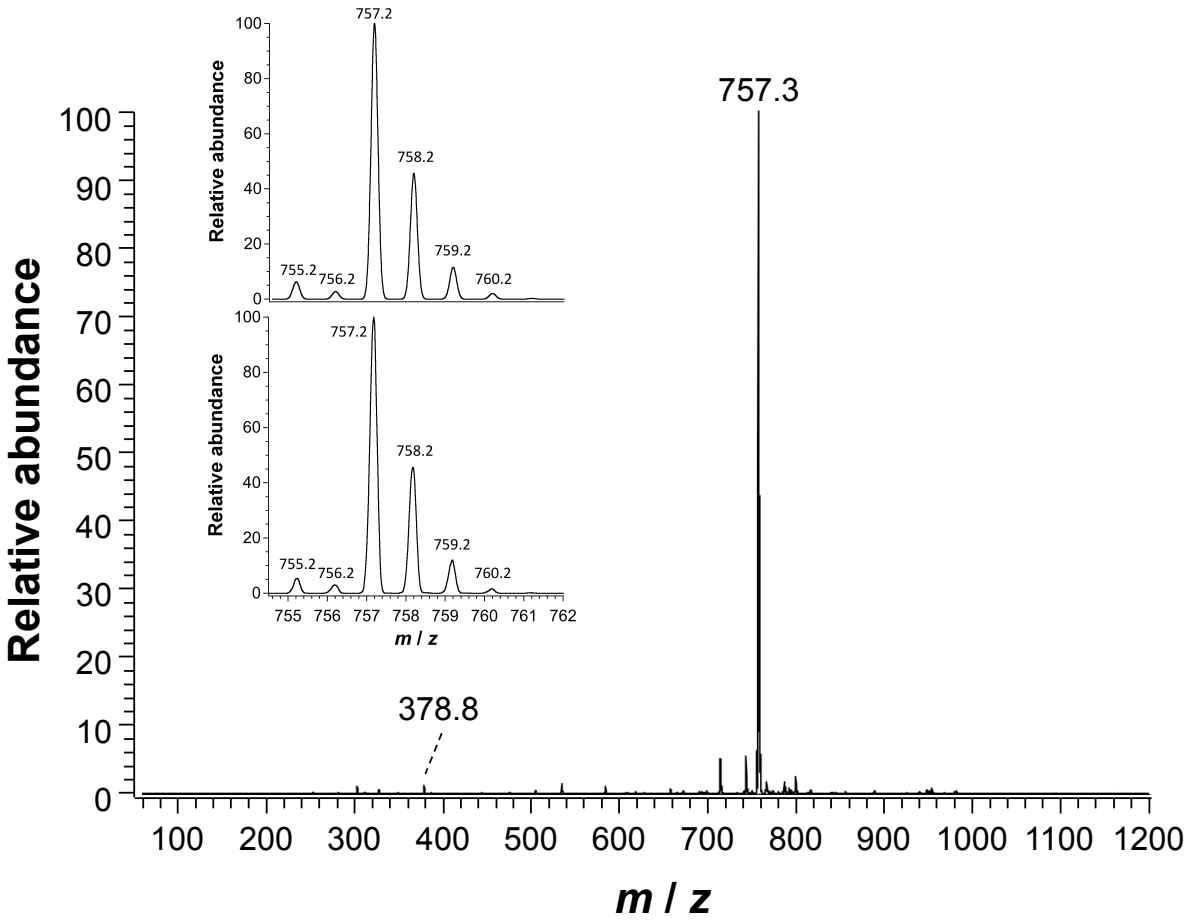

Figure S1. Positive mode ESI-MS spectrum of **2**. The insert reproduces a zoom of the 757 pattern (bottom experimental spectrum, top calculated spectrum).

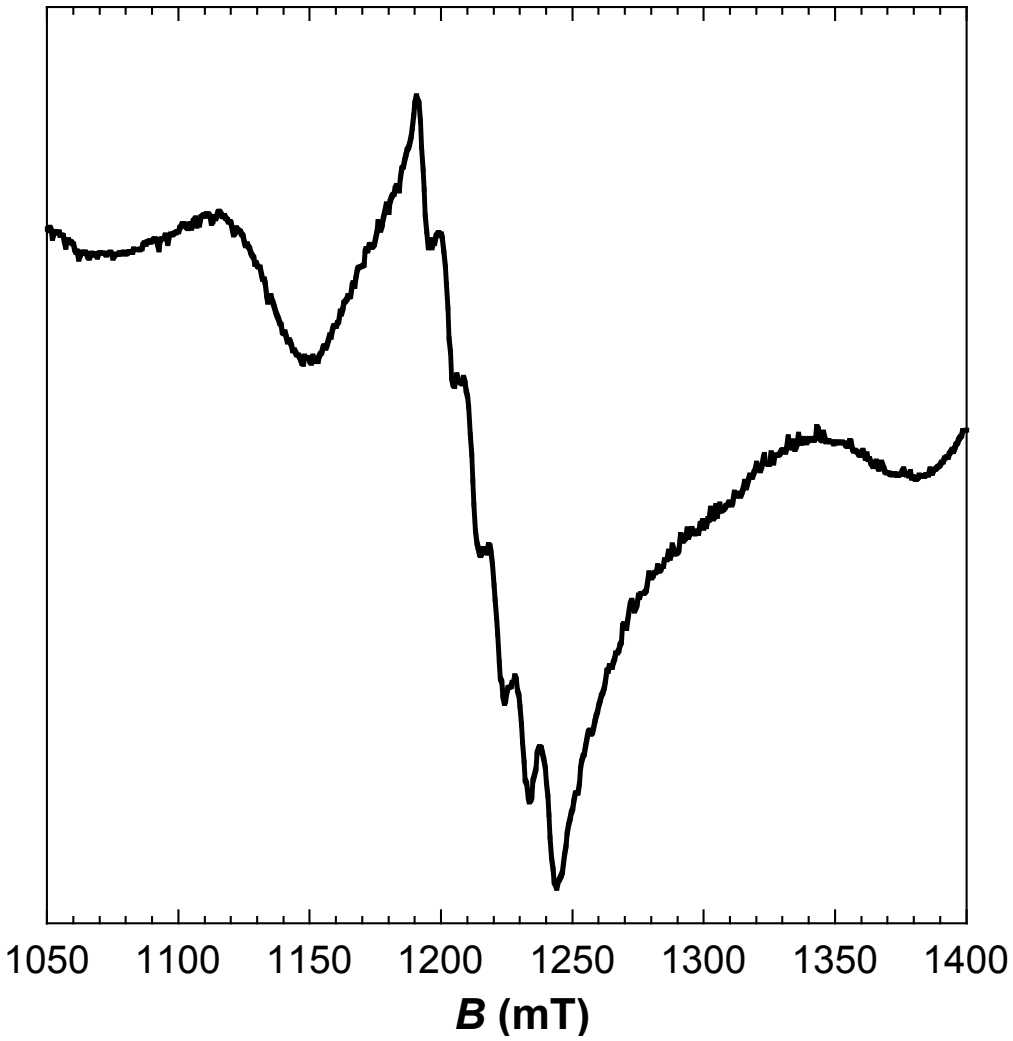

Figure S2. Zoom on the $g_{eff} = 2$ region of the Q-band EPR spectrum recorded at 15 K on a powder sample of **1**. Recording conditions: Microwave frequency = 34 GHz, microwave power = 4.6 mW, modulation frequency = 100 kHz, modulation amplitude = 0.4 mT.

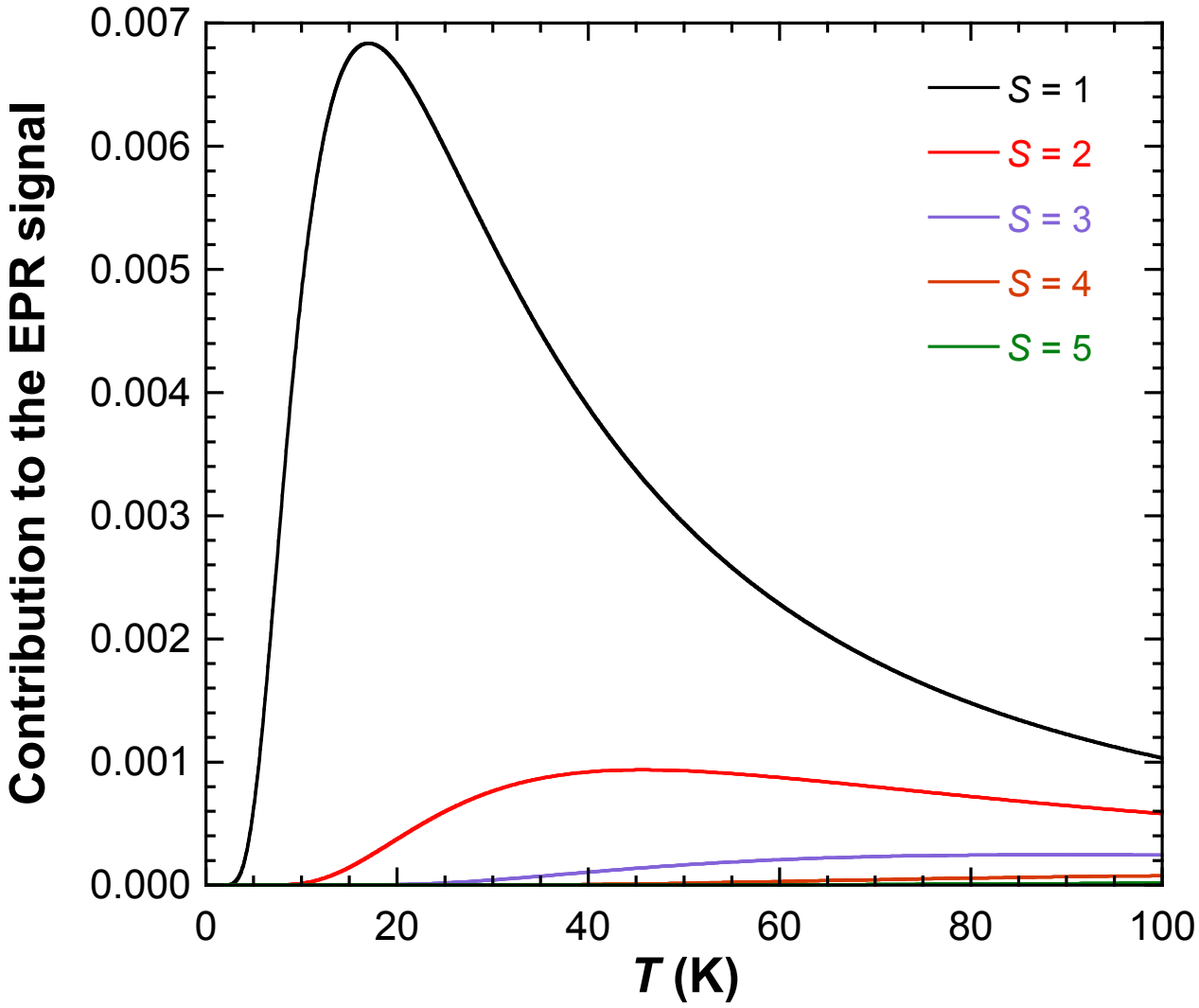

Figure S3. Temperature dependence of the contribution to the total EPR signal of the five paramagnetic excited states of complex **1** (S = 1-5). The curves were calculated assuming $J = 20.0$ cm^{-1} according to the equation given below where T stands for the temperature and k_B is the Boltzmann constant.

$$\text{Contribution to the EPR signal} = \frac{1}{T} \times \frac{\exp\left[-\dfrac{JS(S+1)}{2k_BT}\right]}{\sum_{S_n=0}^{5}(2S_n+1)\exp\left[-\dfrac{JS_n(S_n+1)}{2k_BT}\right]}$$

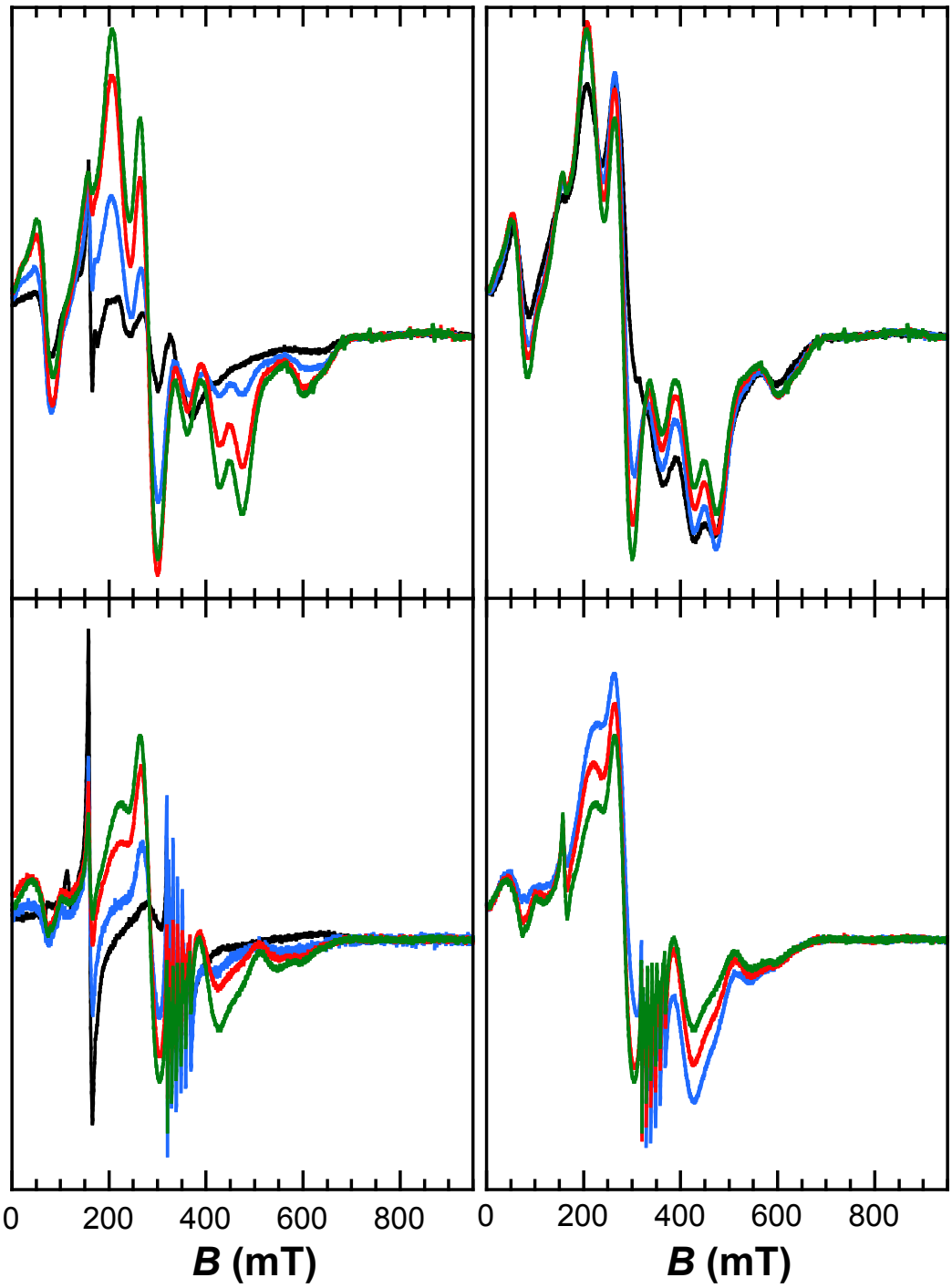

Figure S4. Experimental X-band EPR spectra recorded on a powder (top panels) and a frozen solution (solvent = methanol/toluene in a 1:1 v:v, bottom panels) samples of complex **1**. The two top panels are identical to that of Figure 7 in the main text. Left top panel: T = 20 (black solid line), 30 (blue solid line), 45 (red solid line) and 55 K (green solid line). Right top panel: T = 55 (green solid line), 65 (red solid line), 80 (blue solid line) and 110 K (black solid line). Bottom left panel: T = 10 (black solid line), 20 (blue solid line), 30 (red solid line) and 45 K (green solid line). Bottom right panel: T = 45 (green solid line), 60 (red solid line) and 90 K (blue solid line). Recording conditions: Microwave power = 80 mW, modulation frequency = 100 kHz, modulation amplitude = 0.5 mT.

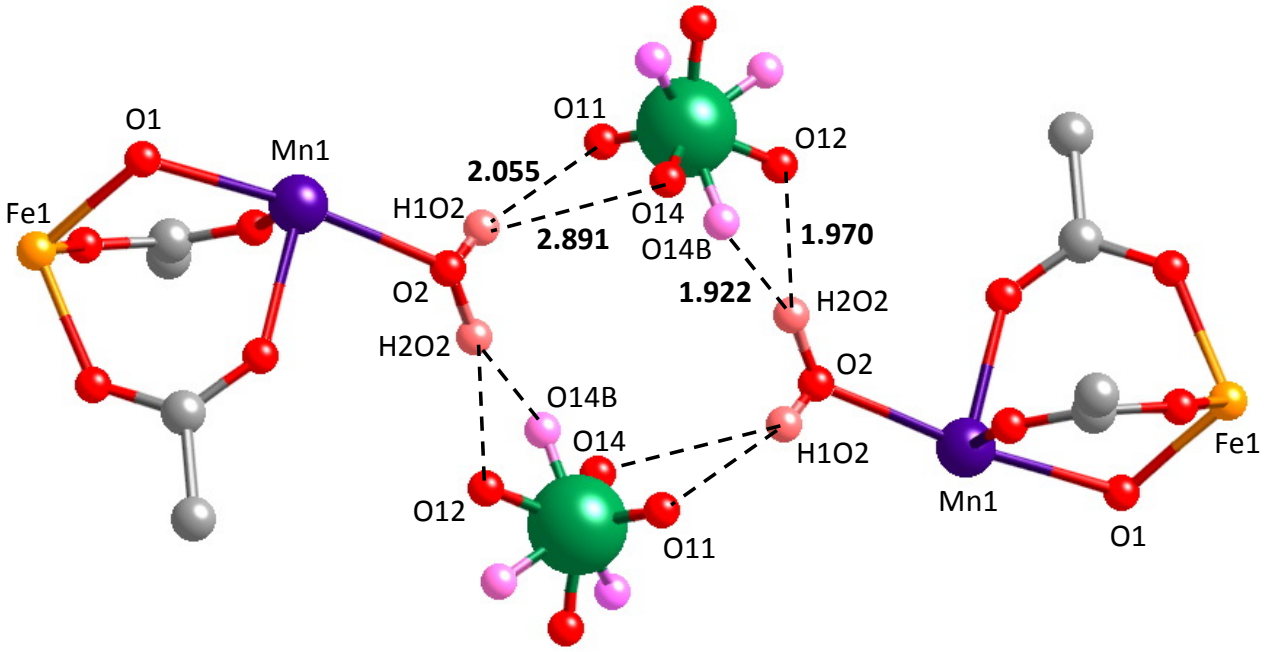

Figure S5. Hydrogen bonds between two $Fe^{III}Mn^{II}$ units through the coordinated water molecules and the perchlorate counter-ions. The separation between the hydrogen atoms of the water molecule and the oxygen atoms of perchlorate anion are indicated in Å. Only distances smaller than 3 Å are reported. The associated angles have the following values: O2–H1O2–O11 = 164.6°, O2–H1O2–O14 = 118.4°, O2–H2O2–O12 = 156.6° and O2–H2O2–O14B = 158.0°. The site occupancies are 1.0 for O11, 0.672 for O12 and O14, and 0.328 for O14B.

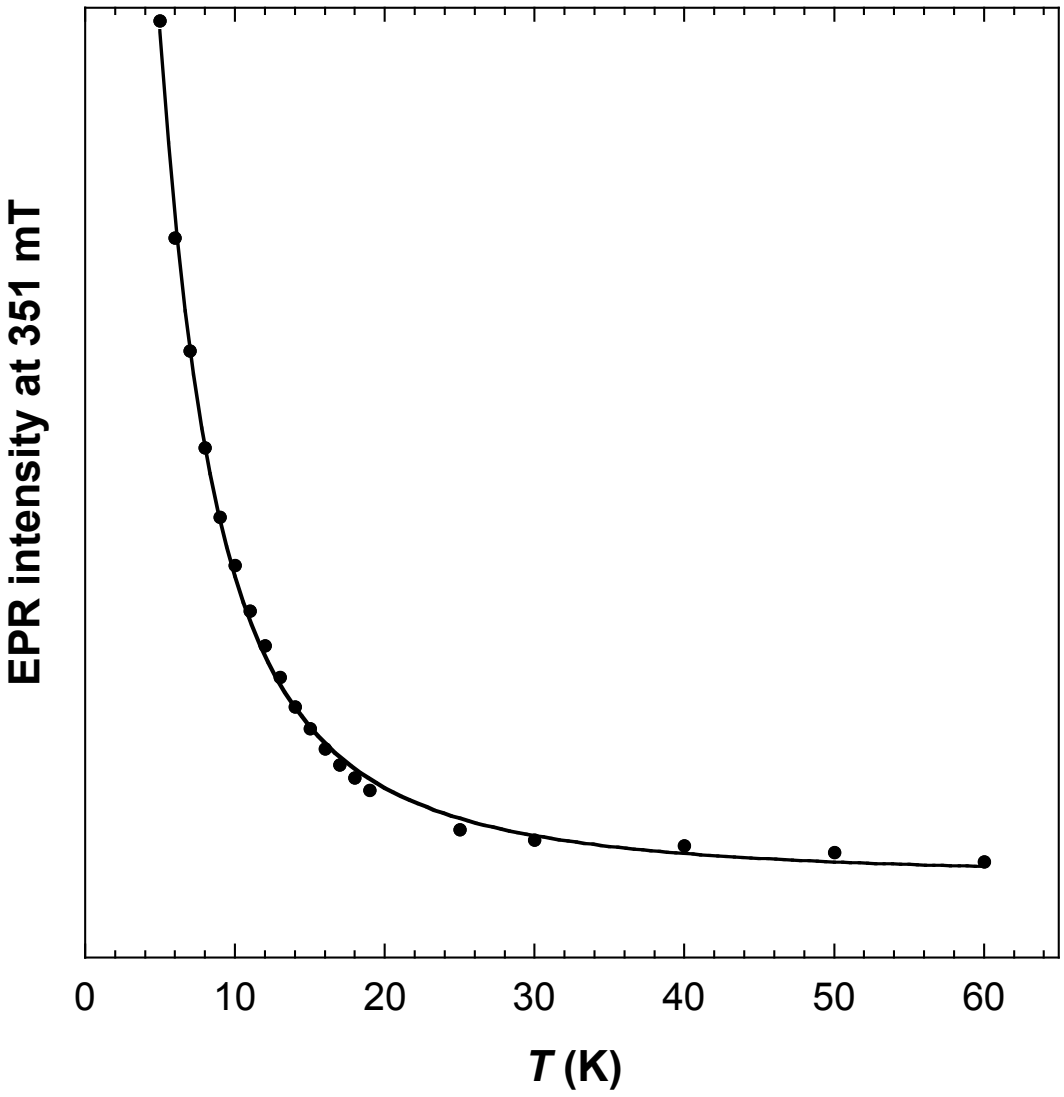

Figure S6. Temperature dependence of the X-band EPR signal of complex **2** measured at 351 mT (black full circles). The black solid line corresponds to the fit of the data according the equation given below that gives the temperature dependence of the Boltzmann population of one Zeeman level of the ground $S_{eff} = 1/2$ state within the strong exchange limit. The obtained J-constant is 6.4 ± 0.4 cm^{-1}.

$$\text{EPR intensity} \propto \frac{1}{T} \times \frac{1}{2 + 4\exp\left[-\frac{3J}{2k_BT}\right] + 6\exp\left[-\frac{8J}{2k_BT}\right] + 8\exp\left[-\frac{15J}{2k_BT}\right] + 10\exp\left[-\frac{24J}{2k_BT}\right]}$$

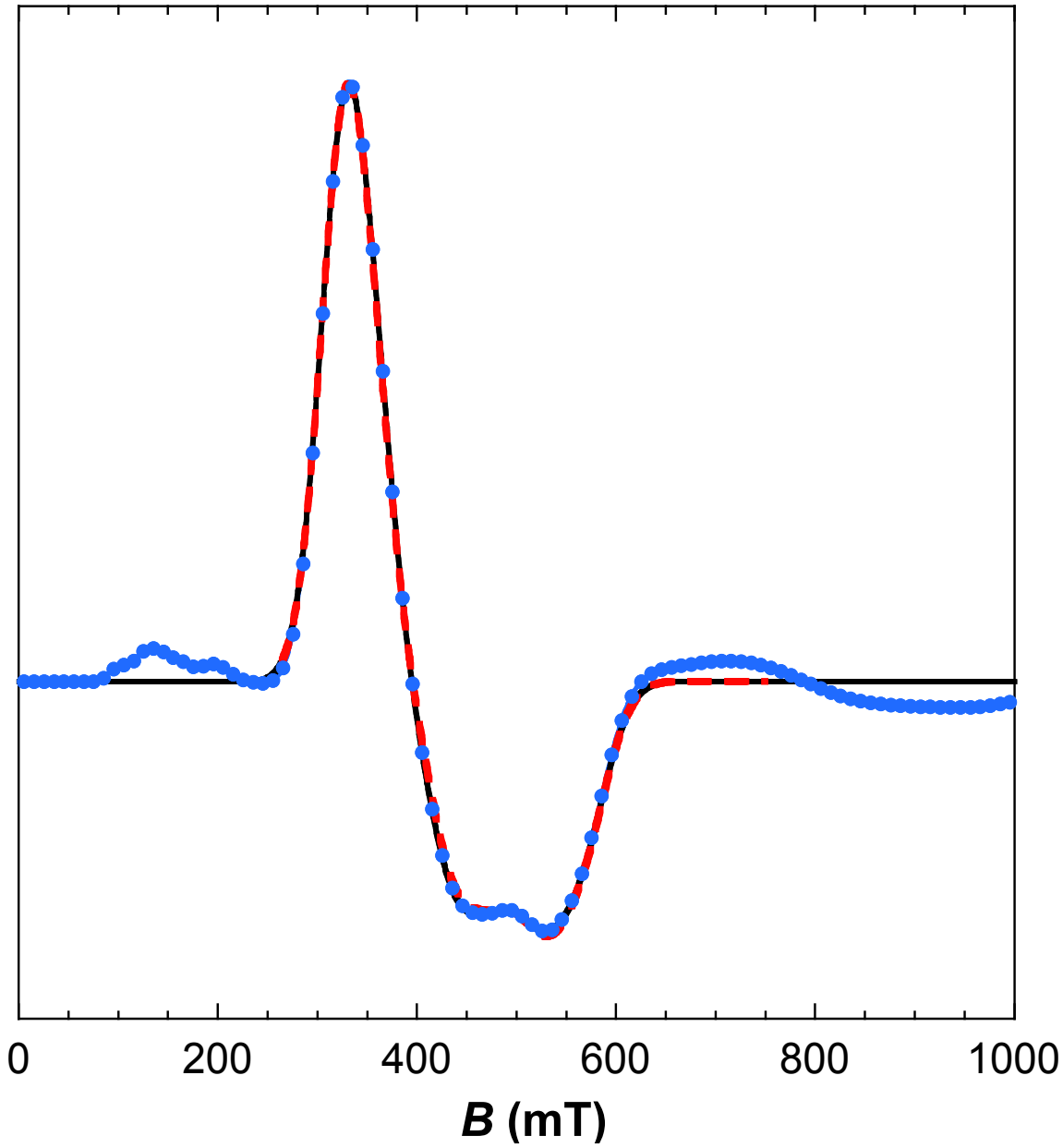

Figure S7. Comparison of the EPR spectra of complex **2** calculated using the XSophe software at 1.4 K (black solid line) and 5 K (blue dots) with the theoretical trace (dashed red line) shown in Figure 9 obtained from the simultaneous simulation of EPR and Mössbauer spectra. The 5 K spectrum has been magnified by a factor of 2.345 to scale the maximum amplitude. Spectra were convoluted using a Gaussian line shape with a full width at half maximum of 645 GHz.

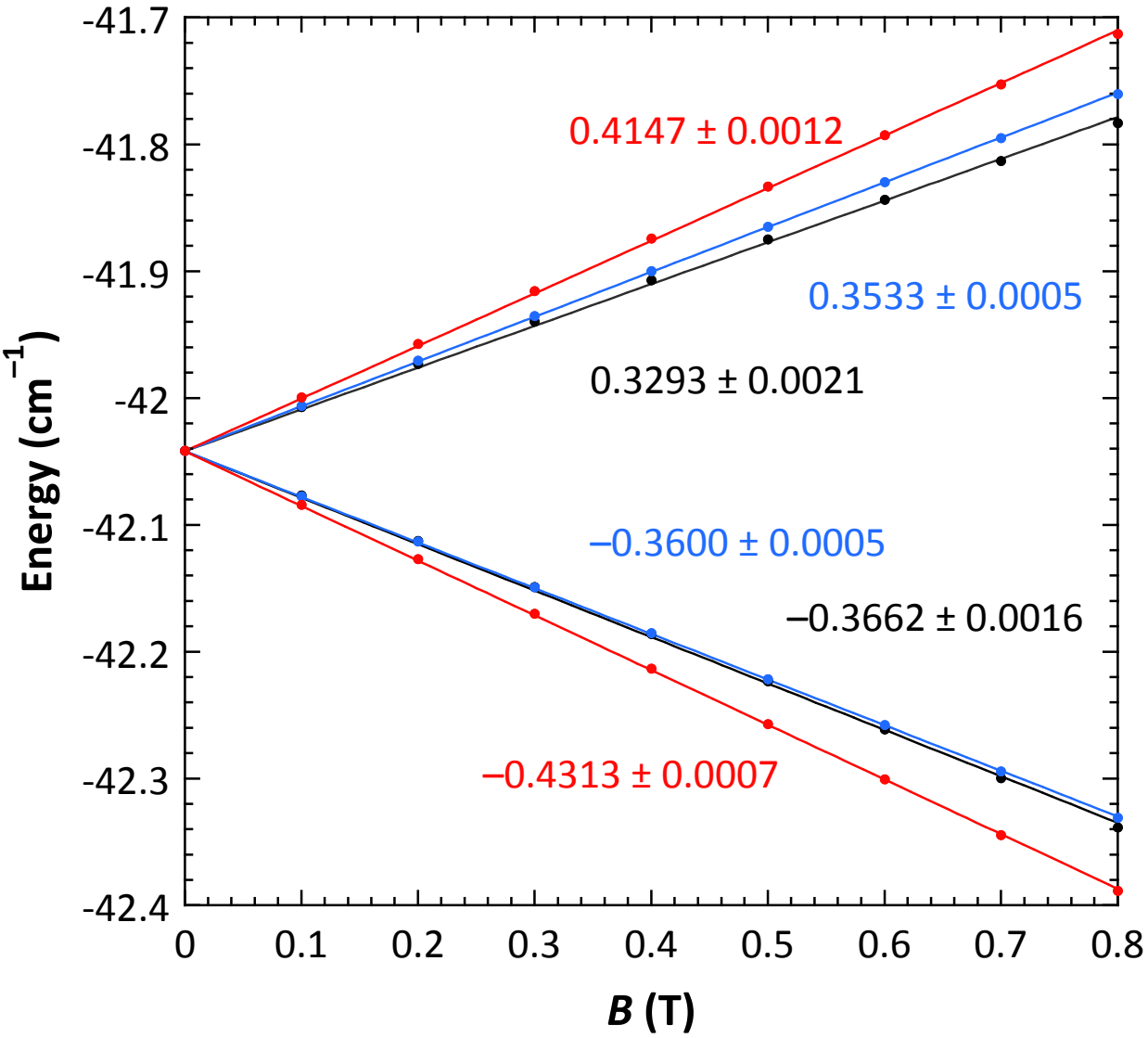

Figure S8. Dependence upon the magnitude of the external magnetic field of the energy of the two levels of the ground Kramers doublet of complex **2** calculated using the spin parameters of Table 4 (full circles). The external field is applied along the *x*- (black), *y*- (blue) or *z*- (red) direction. Solid lines represent the fits obtained assuming a linear dependence and a zero-field energy of 42.042 cm^{-1}. The slopes in cm^{-1}.T^{-1} are indicated along with the errors. The average g_{eff}-values one can determined from the slopes are 1.486 ± 0.010, 1.528 ± 0.002 and 1.809 ± 0.006 for the *x*-, *y*- and *z*-directions, respectively.

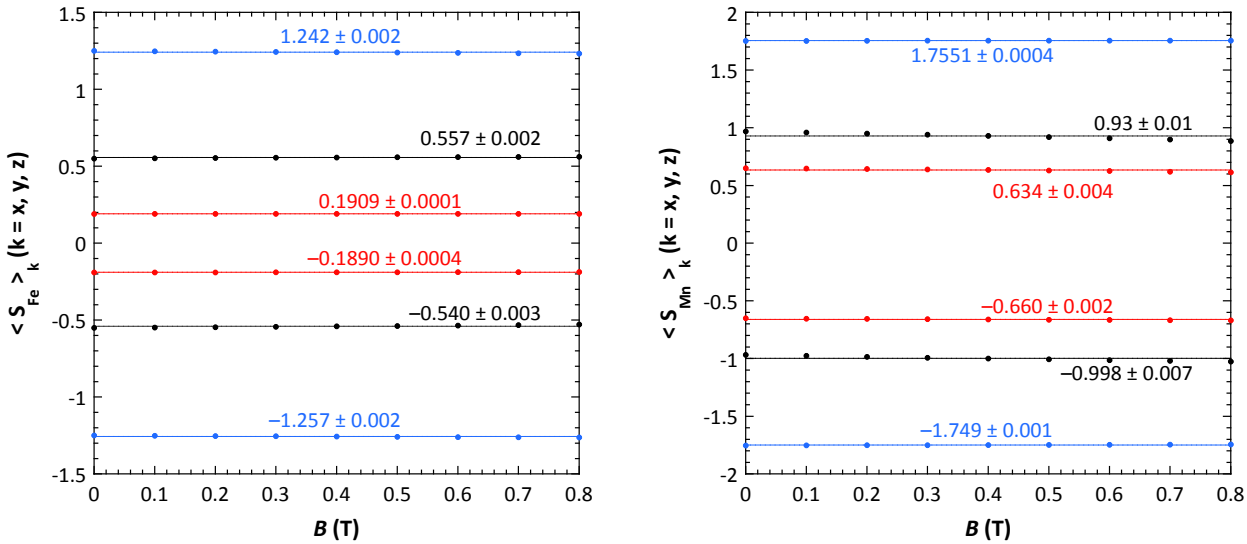

Figure S9. Dependence upon the magnetic field of the spin projections associated to the Fe^{II} (left) and the Mn^{II} (right) sites of the two levels of the ground Kramers doublet of complex **2** calculated using the spin parameters of Table 4 (full circles). The external field is applied along the *x*- (black), *y*- (blue) or *z*- (red) direction. Solid lines represent the fits obtained assuming no-dependence upon *B*.

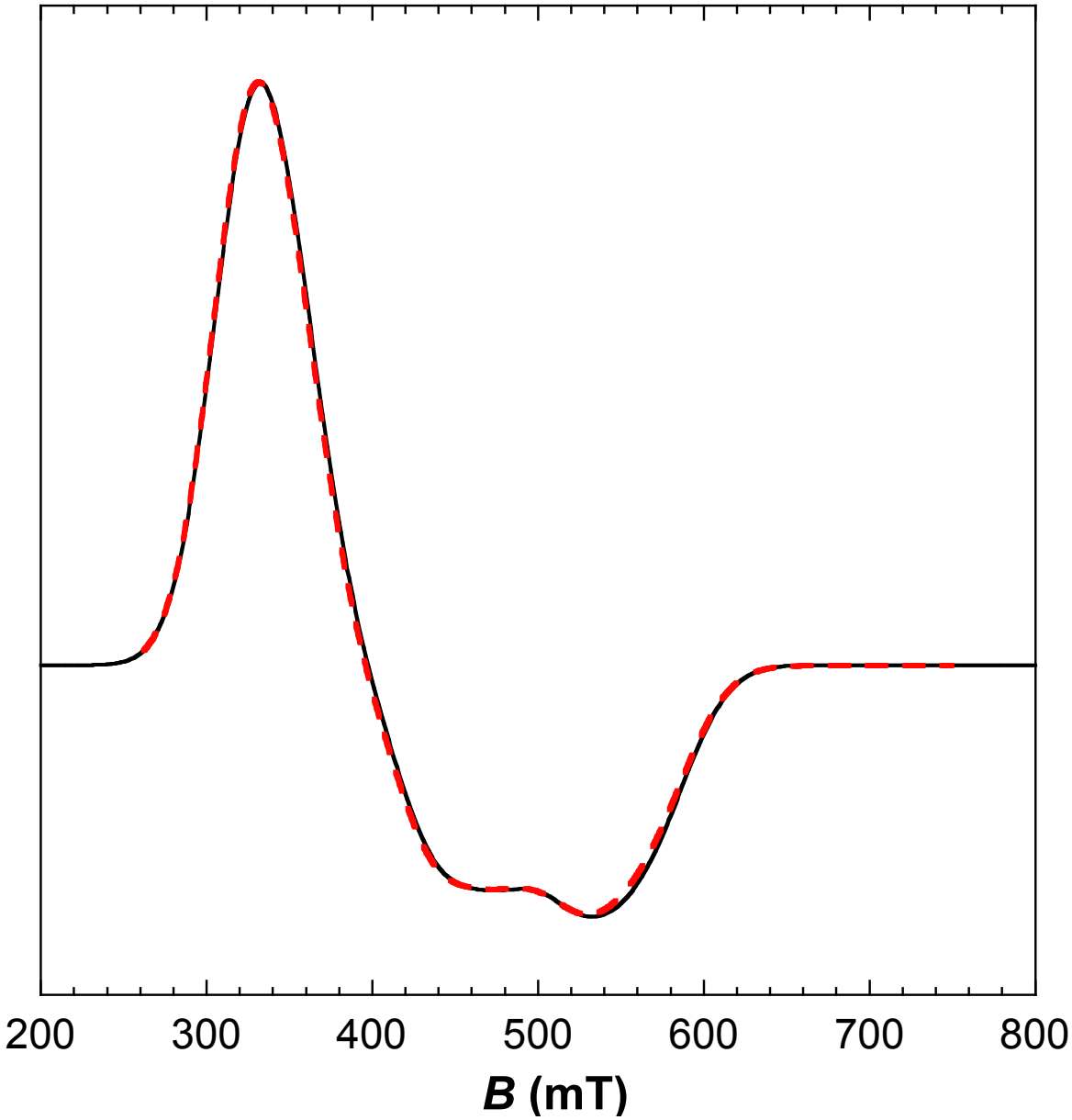

Figure S10. Comparison of the EPR spectra of complex **2** calculated assuming a S_{eff}=1/2 system (solid black line) with parameters listed in Table 5 with the theoretical trace (dashed red line) shown in Figure 9 obtained from the simultaneous simulation of EPR and Mössbauer spectra. Both spectra were convoluted using a Gaussian line shape with a full width at half maximum of 645 GHz.

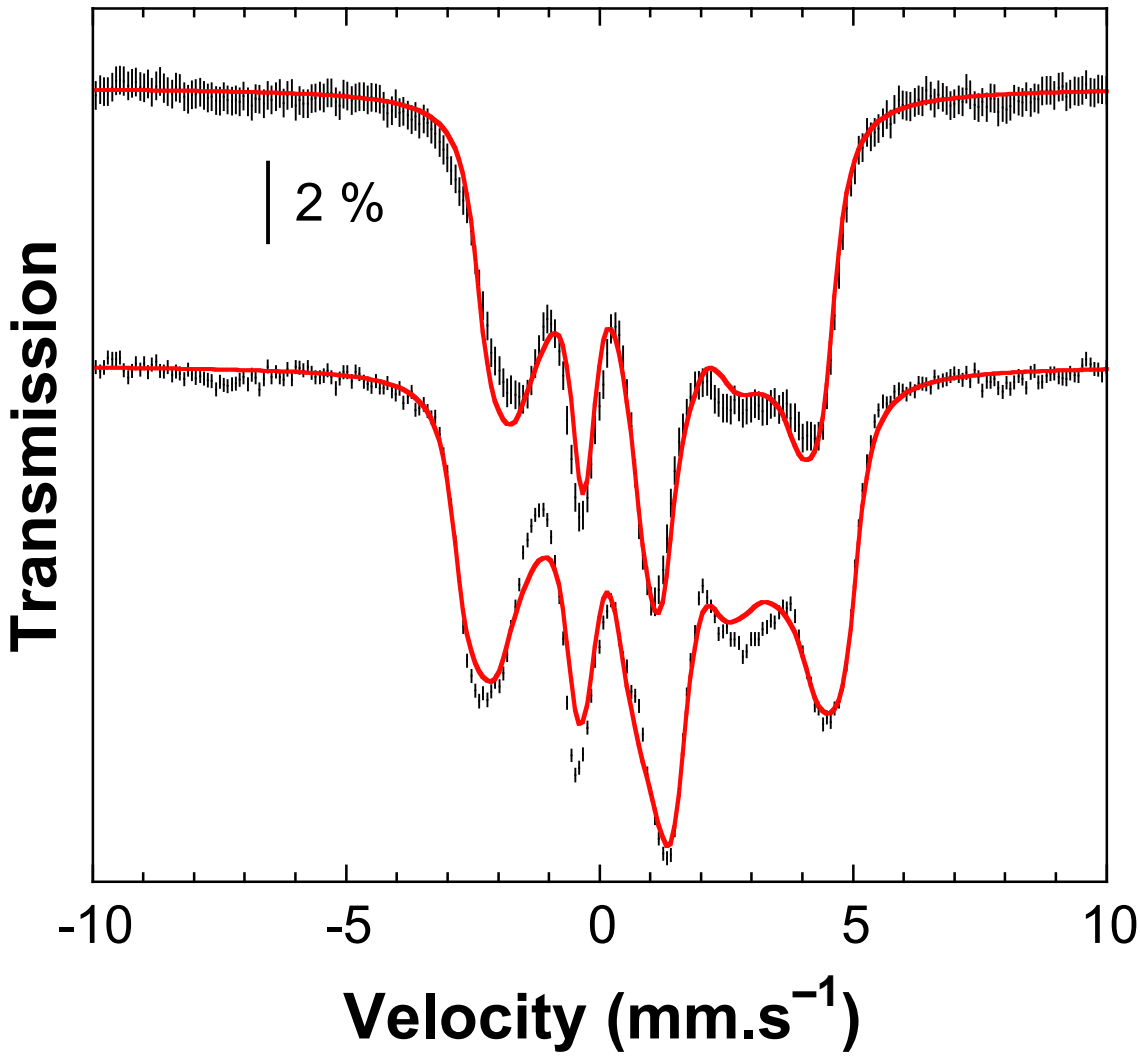

Figure S11. Experimental (dashed black lines) and simulated (solid red lines) Mössbauer spectra recorded on a 100% enriched ^{57}Fe powder sample of **2** at 1.4 K with a 4 T (top trace) or 7 T (bottom trace) external magnetic field applied parallel to the γ-beam. The parameters fixed for the simulation assuming a S_{eff}=1/2 system are: g_{eff} = (1.486, 1.528, 1.809), ΔE_Q = 2.79 mm.s^{-1} and δ = 1.185 mm.s^{-1}. Parameters obtained at the end of the simulation process are: $A_{Fe,eff}$ = (23.4, 17.8, –13.9) T, η = 0.006, ρ = 57°, τ = 23° (χ-angle not relevant due to the axial symmetry of the EFG tensor), Γ_{fwhm} = 0.26 mm.s^{-1}.